Journal of Engineering and Applied Sciences
MEDWELL PUBLICATIONS

Optical Properties and Photo Stability of Different Nanomaterials

[1]Asmaa F. Mansour, [2]Sawsan A. Mahmoud and [1]Mostafa E. Elsisi
[1]*Department of Chemistry, Faculty of Science, Zagazig University, Zagazig, Egypt*
[2]*Egyptian Petroleum Research Institute, Nasr City, Cairo, Egypt*

Key words: Optical properties, hydrothermal method, photo stability, TiO_2 NWA_s, TiO_2 QD_s and TiO_2 NRA_s

Corresponding Author:
Asmaa F. Mansour
Department of Chemistry, Faculty of Science, Zagazig University, Zagazig, Egypt

Page No.: 2279-2286
Volume: 15, Issue 10, 2020
ISSN: 1816-949x
Journal of Engineering and Applied Sciences

Abstract: TiO_2 is one of the common materials used for solar cells, diodes, different types of gas sensors, optoelectronic devices, etc., TiO_2 is widely used in photovoltaic devices due to interesting optical and electrical properties. In this research, there are different types of nano materials were synthesized by different methods, Firstly, TiO_2 nanoparticle has been prepared by sol-gel techniqu. Secondly, TiO_2 nanord and TiO_2 nanowire were synthesized by a hydrothermal method. The thin films of these samples (TiO_2 NP_s-TiO_2 NRA_s-TiO_2 NWA_s) were synthesized on glass substrates via. doctor-blending method. The as-prepared samples were characterized by x-ray diffraction, HR-TEM, FE-SEM and UV-Visible spectrophotometer. X-ray diffraction pattern showed the phase structures of these samples, the Scanning Electron Microscopy (SEM) is used for analysis of morphology and Ultraviolet Visible spectroscopy (UV-Vis) was used to get the degradation degree, the light intensity and the optical absorbance.

INTRODUCTION

With the advent of nanotechnology, in recent past metal oxides nanoparticles, in particular Titanium Oxide (TiO_2) nanoparticles have become a promising material due to their unique properties. TiO_2 besides having wide range of applications such as dye-sensitized solar cells and QD-sensitized solar cells. TiO_2 nanoparticles have been recognized as an important candidate for multiple applications. TiO_2 has good stability under irradiation in solution and low toxicity but there are two serious disadvantages that limit the efficiency of photocatalytic activity of TiO_2 using the light source in the solar spectrum (with 3-5% UV light) they are: the large band gap (3.0 eV of rutile, 3.2 eV of anatase) which suppress its photo-response in visible range due to this it is only active in the ultraviolet range and the fast recombination rate of photoinduced electron (e^-)/hole (h^+) pairs and cannot absorb visible light due to wide band gap of ~3.2 eV. Variety of techniques have been adopted by researchers to synthesize TiO_2 nanoparticles such as chemical vapour deposition (18), sol-gel (19), hydrothermal (20), hydrolysis (21), solvothermal (22), ball milling (23), solution combustion method (24) and many more. These methods provide various morphologies like nanosphere, nanorods and nanowires which having different photocatalytic efficiency. In previous studies, researchers have reported the preparation of TiO_2 nanoparticles using Titanium Tetrachloride ($TiCl_4$) and titanium (IV) isopropoxide as a precursor. The physical properties of TiO_2 depend on many factors such as crystal structure, size, morphology and the prepartion methods.

TiO_2 exists in three crystallographic phases namely rutile, anatase and brookite. In general, anatase phase of TiO_2 NPs is found to be active and possess high photocatalytic efficiency compared to rutile phase due to electron hole pair recombination rate. Photocatalytic process involves the electron in the Valance Band (VB) were excited towards the Conduction Band (CB) by illuminating the UV light. The photocatalytic effect of TiO_2 nanorods were studied on the degradation of Methyl orange in aqueous solution. They also synthesized single-crystal TiO_2 nanowire arrays on FTO glass under mild hydrothermal conditions. The functional nanostructured photoanodes such as one-dimensional nanostructures (nano rods (2), nanowires (3)). In this study, the sol-gel method uses a titanium (IV) isopropoxide and ethanol absolute which is based mainly on the hydrolysis and condensation of metal alkoxides at low temperature (12). The sol-gel dip coating is the simplest, economical method and has advantages such as TiO_2 is easily toodeposited on the glass substrates. In this research, (rutile/anatase) TiO_2 nanorod/ nanowire arrays were synthesized via the hydrothermal method. The main objective of this paper is tostudy the crystallization of TiO_2 thin films of different nanomaterials (TiO_2 NP_s, TiO_2 NRA_s and TiO_2 NWA_s) deposited by doctor- blending technique as a function of calcination temperatures. Structural, morphological and optical properties with annealing temperature are investigated by X-Ray Diffraction (XRD), Field Emission Scanning Electron Microscopy (FE-SEM), Photo Stability (PS), High Resolution Transmission Electron Microscope (HR-TEM) andUV-VIS spectrophotometer.

MATERIALS AND METHODS

Experimental: Titanium (IV) isopropoxide (97%, Aldrich), ethanol absolute (Adwic), Sodium Hydroxide (Aldrich), Triton-X100 (Aldrich), Nitric acid (Adwic), Hydrochloric Acid (Adwic) and deionized water.

Synthesis of TiO_2 quantum dots: Titanium (IV) isopropoxide (TIP) [Ti [OCH $(CH_3)_2]_4$ was used as the precursor for the sol-gel synthesis of nanoparticle TiO_2 catalysts. The sol-gel method include hydrolysis and condensation process of Titanium (IV) isopropoxide in aqueous media under acidic condition. The procedure used is followed by preparing two solution: in solution A, TIP added to ethanol absolute at volume ratio (1:3) under continuous stirring for 30 min until a homogenous white yellow solution produce. In solution B, deionized water added to ethanol absolute at volume ratio (1:4), nitric acid (HNO_3) as N_2 atmosphere is mixed well to solution by drop wise until the pH value approaching about (2) under magnetic stirring for 1 h at room temperature for restrain the hydrolysis process of the solution. Finally, the contents of beaker B was added slowly into beaker A and aged under vigorous stirring for 2 h. The gel is dries at 80°C in water path for 1 h until most ethanol evaporate, then the produced mixture is dries overnight (for 24 h) in a regular laboratory oven at 80°C. Finally, the dry amorphous gelwas transformed into anatase-crystalline TiO_2 QD_s by calcination at 400°C for 2 h.

Synthesis of TiO_2 nanorod arrays (TiO_2 NRAs): The rutile TiO_2 nanorod arrays were synthesized by a hydrothermal technique using Titanium (IV) Isopropoxide (TIP) as a Ti precursor. Taking, deionized water was mixed with concentrated hydrochloric acid (37%) then, followed by stirring at standered condition for 5 minute, then titanium (IV) isopropoxide was added drop by drop to the mixture. After stirring for another 5 min, the resulting clear transparent solution was transferred to a teflon-lined stainless steel autoclave (400 mL volume) and the hydrothermal synthesis was conducted at 150°C for 20 h in a regular laboratory oven. After synthesis, the autoclave was cooled to room temperature and the white precipitate is collected then, washed using deionized water several times, dried at 80°C for 12 h and calcined at 500°C for 2 h to increase the crystallinity.

Synthesis of TiO_2 nanowire arrays (TiO_2 NWAs): TiO_2 nanowires were prepared using hydrothermal method. In a typical preparation procedure, The prepared anatase TiO_2 white powders were dispersed in 10 m NaOH aqueous solution under ultrasonic treatment for 30 min then the mixture placed into a Teflon-lined autoclave of 400 mL capacity (the autoclave was filled with up to 80% of the total volume), sealed into a stainless steel tank and maintained at 200°C for 24 h without shaking or stirring during the heating. After the autoclave was naturally cooled to room temperature, the obtained sample was sequentially washed with dilute HCl aqueous solution and deionized water for several times until the pH value approaching about 7. Finally, the sample was dried at 80-85°C for 12 h and calcined at 400°C for 2 h.

Fabrication of TiO_2 nanoparticle films: For optical properties measurements, TiO_2 NWA_s, TiO_2 NP_s and TiO_2 NRA_s films with 0.05 g cm^{-2} thickness were prepared from the various TiO_2 nanomaterials powders. The samples of TiO_2 nanomaterials films were directly deposited onto glass substrates by doctor-blading method using dispersion of 0.2 g TiO_2 powder in ethanol solution, the surfaces of the glass substrates were cleaning for 30-60 min using ultrasonicator before spreading the film then the substrates were dried in air. To controlthe thickness of the film the boundaries of glass substrates, adhesive tapes were used on the glass surface in order to delimit the active area of the film or were covered with scotch tape. To produce the film of TiO_2 QD_s, powder was first dispersed in Triton-X100 and ethanol but to prepared

TiO_2 NWA_s and TiO_2 NRA_s films, powder was first dispersed in Triton-X100 and acetic acid until get homogeneous pastes of these different nanomaterials. The paste was spread on the glass surface by using a glass slide, then the suspended powder was added as drops at the middle of the substrate and was spread to form a thick film. Then kept the layer at room for 30 min temperature then drying at hot plate at 300°C for 5 min.

Methods of analysis: Several techniques were used to characterize the surface of prepared materials.

X-Ray Diffraction (XRD): X-ray diffraction patterns were recorded with a Pan Analytical Model X' Pert Pro which was equipped with CuKα radiation (λ = 0.1542 nm), Ni-filter and general area detector. An accelerating voltage of 40 kV and an emission current of 40 mA were used. The diffract grams were recorded in the 2θ range of 0.5-70°.

Fourier Transform Infrared spectroscopy (FTIR): Fourier Transform Infrared (FTIR) spectroscopy Fourier Transform Infrared spectroscopy (FT-IR) of the prepared samples was measured using Nicolet Is-10 FT-IR spectrophotometer adopting KBr technique; thermo fisher scientific. For all samples, the KBR technique was carried out approximately in a quantitative manner since the weight of sample and that of KBr, were always kept constant.

High Resolution Transmission Electron Microscopy (HR-TEM): High Resolution Transmission Electron Microscopy (HR-TEM) images for the prepared samples were recorded on a JEOL JEM-1230 electron microscope operating at an acceleration voltage of 120 kV. The samples for TEM measurements were prepared by dropping a carbon-coated copper grid with suspended of materials in methanol HPLC which was pre-sonicated for 15 min.

Field Emission Scanning Electron Microscope (FE-SEM): Field Emission Scanning Electron Microscope (FE-SEM) s used to analyze the morphology, particle size and shape of the materials. For the prepared samples were recorded on a JSM-7500F electron microscope operating at an acceleration voltage of 30 kV.

UV-Vis absorption spectroscopy: Optical absorption spectra of the samples were measured using Ultraviolet-Visible absorption spectroscopy (Spectro UV-Vis 2800, USA). Barium sulfate solution was used as a reference material.

RESULTS AND DISCUSSION

Figure 1 shows the X-Ray Diffraction (XRD) spectra of the titanium oxide nanoparticles at 400°C, Cupper sulfide and Cupper Nickle nanoparticles. XRD spectrum of TiO_2 QD_s sample, shows that the anatase phase is formed with the broad peaks. All diffraction peaks for the sample, show the anatase phase with tetragonal structure is formed and all diffraction peaks were in good agreement with JCPDS No. 21-1272. The diffraction peaks located at 2θ are 25.21°, 37.60°, 47.94°, 51.45°, 53.92°, 55.01°, 62.59° and 65.42° corresponding to the (101), (004), (200), (105), (211), (204), (116) and (215) lattice planes, respectively. Further, we have observed that without recrystallization results into amorphous polymorphs of TiO_2. The estimated value of crystalline size of the sample is 7.23 nm. The crystallite size was calculated using Sherrer equation as follows[1]:

$$D = K\lambda/\beta\cos\theta$$

Where:

D	:	The crystallite size
K	:	A dimensionless shape factor has a typical value of about 0.9
λ = 1.54A°	:	The X-ray wavelength
β	:	The line broadening at half the maximum intensity (FWHM)
θ	:	The Bragg's diffraction angle

Figure 2 shows the FTIR spectra of TiO_2 QD_s, TiO_2 NR and TiO_2 NW. Curves a represent FTIR spectra for sample TiO_2 QD_s calcined at 400°C. The absorption band observed in the ranges of 400-800 cm^{-1} is associated to the bending vibration (O-Ti-O) bonds in the TiO_2 lattice[2-4] which confirms the presence of TiO_2 as crystalline phase. The sharp peak at 1620 cm^{-1} refer to characteristic bending vibration of –OH group[3-5]. A broad absorption peak observed in the ranges 3200 to 3800 cm^{-1} is due to the interaction of hydroxyl group of water molecule with TiO_2 surface[3-6]. The intensity of higher absorption bands decreases with calcination temperature which is inferred that the removal of water molecules from sample and particle growth.

Optical properties: The FT-IR spectra of TiO_2 nanorod is shown these figure. It is believed that the broad absorption peak at 3000-3600 cm^{-1} is attributed to the fundamental O-H stretching vibration of hydroxyl group[5] The weak band occurs at 1615-635 cm^{-1} correspond to O-H bending vibration of hydroxyl

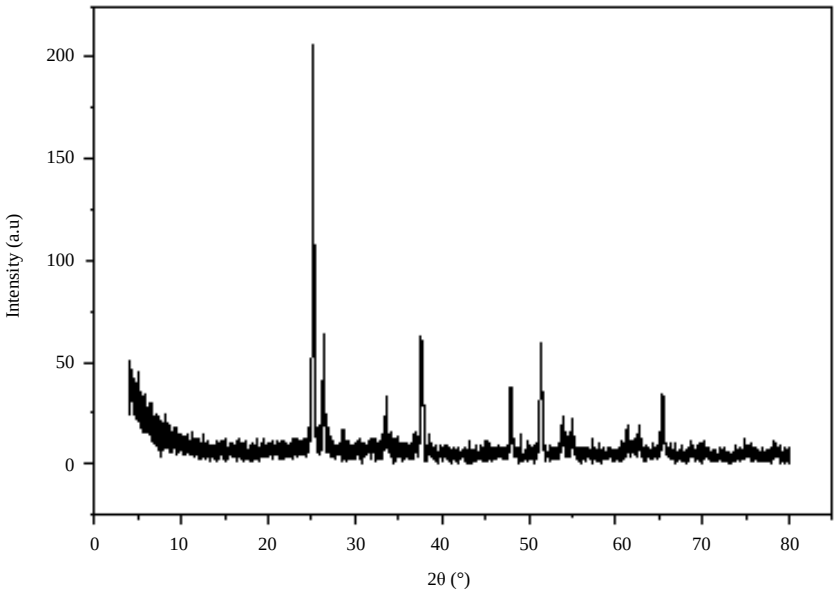

Fig. 1: XRD spectra of TiO_2 QD_s at 400°C (TiO_2 at 400°C)

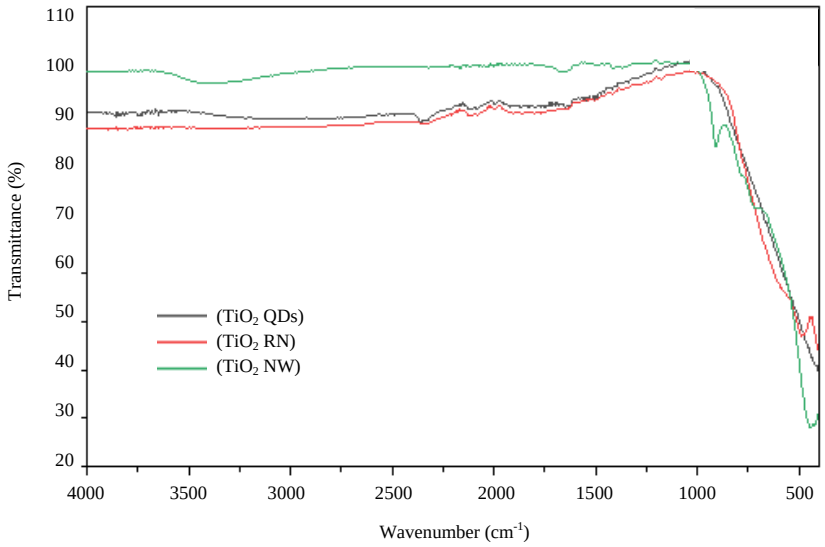

Fig. 2: FTIR spectra of TiO_2 QD, TiO_2 NRA_s and NWAs

group due to chemically adsorbed water molecules[6]. The peak around 800 cm^{-1} was assigned to the Ti-O stretching band[7] confirms the formation of TiO_2[8].

Shows the FTIR spectra of TiO_2 nanowirehas vibration bands at 800-1200 cm^{-1}which are characteristic of the O-Ti-O network. The TiO_2 nanowire showed one broad band near 3400 cm^{-1} which correspond to the water molecules and hydroxyl groups adsorbed on the surfaces and another peak at 1650 cm^{-1} is due to O–H bending vibrations of adsorbed water molecules. TiO_2 nanowire was prepared totally in anatase phase, so, The Ti-O-Ti stretching vibration band near 895 cm^{-1} for TiO_2 nanowire[9]. Figure 3 shows High Resolution Transmission Electron Microscopy (HR-TEM) of the as-prepared and calcined samples. Figure 3a, b the as-prepared TiO_2 QD contains amorphous structure as indicated by XRD. TiO_2 QD after calcination to400°C the particle size distribution assembled to aggregates; the crystallite size ranged 7.36-9.50 nm. Figure 3c, d TiO_2 NRA_s after calcination to 500°C the crystalline width ranged 31.48-81.48 nm and the crystalline length ranged from 202.31-900.63 nm and TiO_2 NWA_s was calcinated

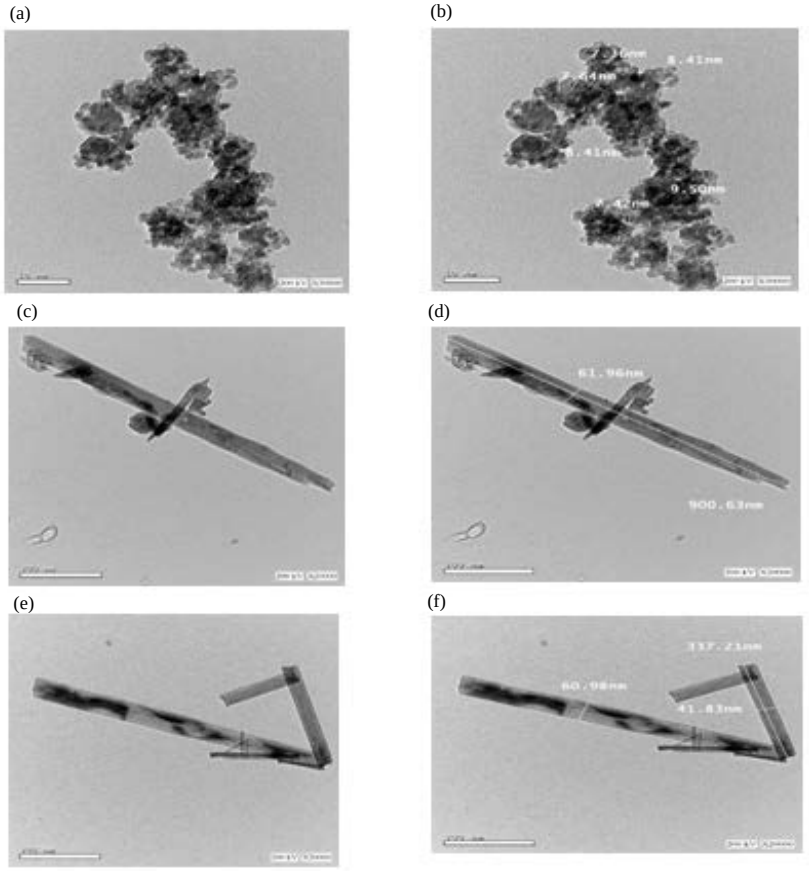

Fig. 3(a-f): HR-TEM of (a-b) TiO_2QD_s, (c-d) TiO_2 NRA_s and (e-f) TiO_2 NWA_s

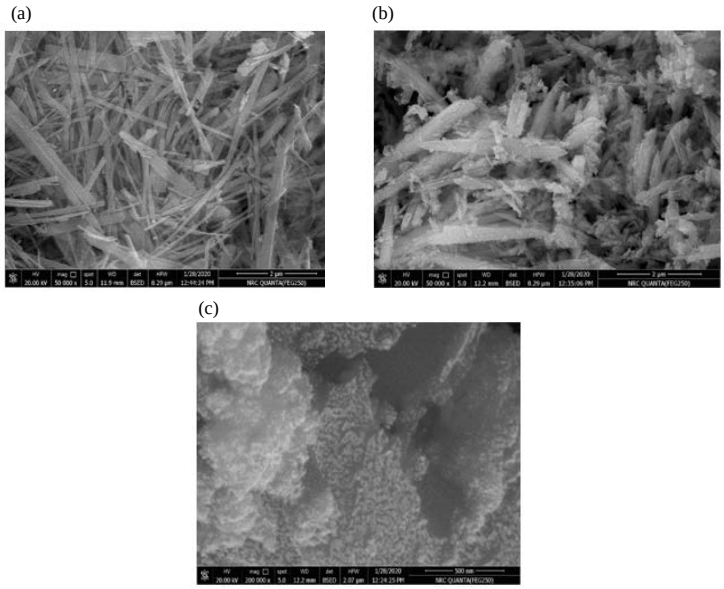

Fig. 4(a-c): FE-SEM of (a) TiO_2 NWA_s, (b) TiO_2 NRA_s and (c) TiO_2 QD_s

at 400°C shows clear wires structures and the wires have a length of 735.20 and 40.18 nm diameter shown in Fig. 3e, f. Figure 4 shows the FE-SEM images for the TiO_2 QD, TiO_2 NRA_s and TiO_2 NWA_s. From FE-SEM

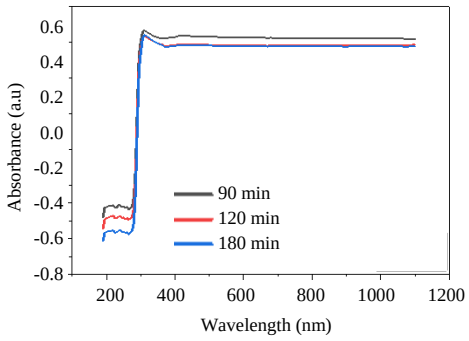

Fig. 5: Absorbance spectra of synthesized TiO_2 QD_s at 90, 120 and 180 min

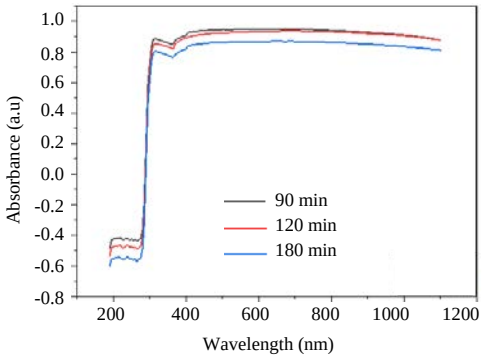

Fig. 7: Absorbance spectra of synthesized TiO_2 NWA_s at 90, 120 and 180 min

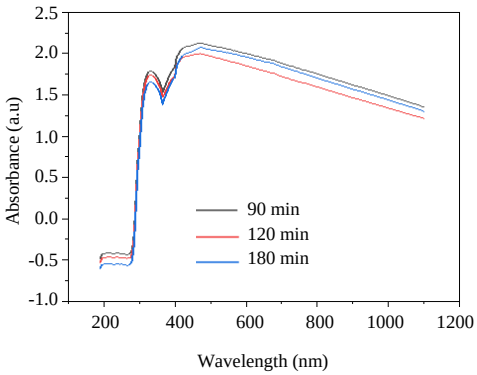

Fig. 6: Absorbance spectra of synthesized TiO_2 NRA_s at 90, 120 and 180 min

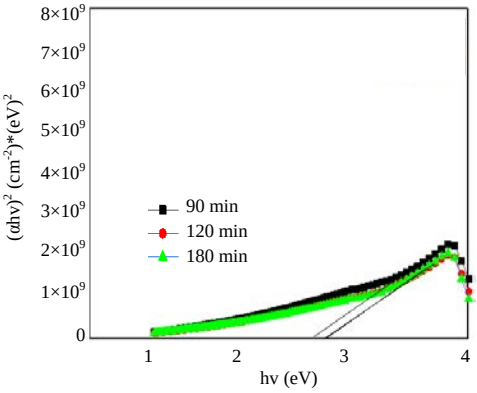

Fig. 8: Optical band gap of synthesized TiO_2 QD at 90, 120 and 180 min

images of samples, Fig. 4c it is found the particles for TiO_2 QD are homogeneous and almost irregular in shape. From the sample at 400°C, it is found that particle size is increased and is highly agglomerated[9]. Figure 4b show that particle size of the sample in the range (7.36-9.50 nm), shows the micrographs of TiO_2 nanorods, TiO_2 nanorods are reunited together and the uniform diameters of nanorods is about 281.4 nm with length of about 500 nm and Fig. 4a show that TiO_2 NWA_s morphology and indicates both variable lengths ~510 nm and uniform diameters in range 49.55-80.21 nm.

Figure 5a shows the UV–vis absorption spectra and photostability for samples at different exposure time of light. It is seen that absorption edge of TiO_2 QD_s calcined at 400°C,TiO_2 NRA_s and TiO_2 NWA_s. The absorption edges for TiO_2 QD_s calcined at 400°C were decreasing by increasing exposure time to180 min but samples at 120 and 180 min have the same absorption edge due to photostability of samples. Figure 6 shows the UV–vis absorption spectra and photostability for samples at different exposure time of light. It is seen that absorption edge of TiO_2 NRA_s. The absorption edges for TiO_2 NRA_s were decreasing by increasing exposure time to 180 min due to photostability. Figure 7 shows the UV-vis absorption spectra and photostability for samples at different exposure time of light. It is seen that absorption edge of TiO_2 NWA_s. The absorption edges for TiO_2 NRA_s were decreasing by increasing exposure time to 180 min due to photostability. To know the nature of band gap, we have made detailed calculation of band gap using Tauc formula:

$$(\alpha hv)\ n = A\ (hv\text{-}Eg)$$

Where:

α : The absorption coefficient
hv : The energy of photon
E_g : The energy gap
n : The nature of the transitions

The term n is taken 2 for direct transition and ½ for an indirect transition. The band gap is determined by plotting $(\alpha hv)^n$ versus energy of photon and tangent drawn to the curve intersect the energy axis at α = 0. Figure 8 shows the Tauc plot of TiO_2 QD_s calcined at 400°C for direct band transition and the estimated direct band gaps of TiO_2 QD_s calcined at 400°C at exposure times 90, 120

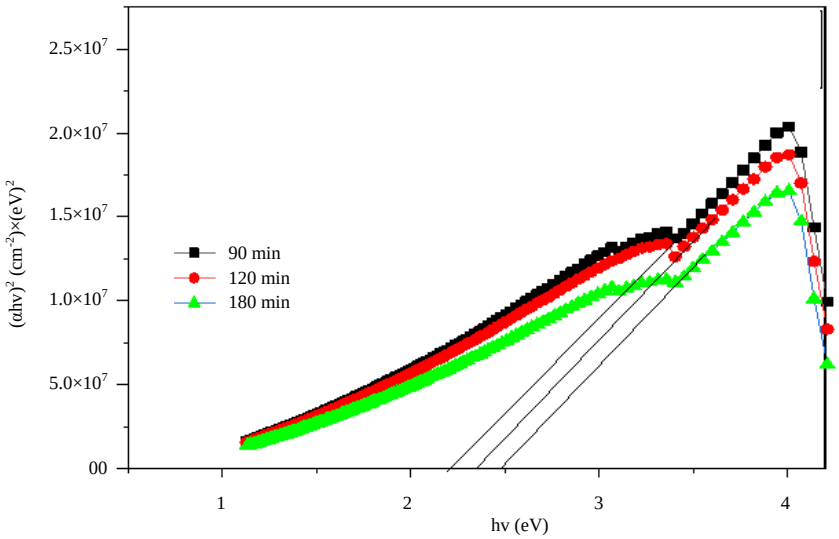

Fig. 9: Optical band gap of synthesized TiO_2 NRA_s at 90, 120 and 180 min

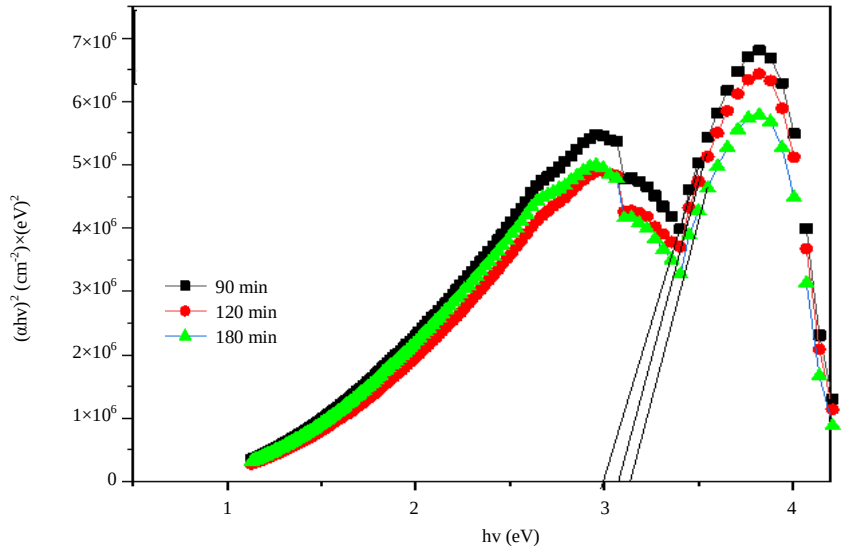

Fig. 10: Optical band gap of synthesized TiO_2 NWA_s at 90, 120 and 180 min

and 180 min are 2.68, 2.8 and 2.8 eV, respectively. Figure 9 shows the Tauc plot of TiO_2 NRA_s for direct band transition and the estimated direct band gaps of TiO_2 NRA_s at exposure time's 90, 120 and 180 min are 2.19, 2.34 and 2.47, eV respectively. Figure 10 shows the Tauc plot of TiO_2 NWA_s for direct band transition and the estimated direct band gaps of TiO_2 NWA_s at exposure time's 90, 120 and 180 min are 3, 3.07 and 3.13 eV, respectively.

CONCLUSION

Titanium dioxide nanoparticle was synthesized by sol-gel method. Titanium dioxide nanorod and Titanium dioxide nanowire were synthesized by a hydrothermal method. Absorbance spectra for TiO_2 NRA_s and TiO_2 NWA_s is decreasing by in increasing exposure time from (90-180 min) under light of photostabilizer.

Optical band gap in direct allowed transition for TiO_2 NRA_s and TiO_2 NWA_s increasing by increasing exposure time from (90-180 min) under light of photostabilizer. Absorbance spectra for TiO_2 QD_s is remains stable by increasing exposure time at 120 and 180 min under light of photostabilizer.

Optical band gap in direct allowed transition for TiO_2 QD_s and is remains stable by increasing exposure time at

120 and 180 min which are 2.8 and 2.8 eV, respectively under light of photostabilizer. TiO_2 QD_s is more stable than TiO_2 NRA_s and TiO_2 NWA_s. TiO_2 QD_s can be used as a working electrode in solar energy conversion due to it has a higher stability and higher efficiency than other nanomaterials.

REFERENCES

01. Horti, N.C., M.D. Kamatagi, N.R. Patil, S.K. Nataraj, M.S. Sannaikar and S.R. Inamdar, 2019. Synthesis and photoluminescence properties of titanium oxide (TiO_2) nanoparticles: Effect of calcination temperature. Optik, Vol. 194, 10.1016/j.ijleo.2019. 163070
02. Mathew, S., A.K. Prasad, T. Benoy, P.P. Rakesh and M. Hari *et al*., 2012. UV-visible photoluminescence of TiO_2 nanoparticles prepared by hydrothermal method. J. Fluoresce., 22: 1563-1569.
03. Chen, Y.F., C.Y. Lee, M.Y. Yeng and H.T. Chiu, 2003. The effect of calcination temperature on the crystallinity of TiO_2 nanopowders. J. Crystal Growth, 247: 363-370.
04. Chen, H., D. Chen, L. Bai and K. Shu, 2018. Hydrothermal synthesis and electrochemical properties of TiO_2 nanotubes as an anode material for lithium ion batteries. Int. J. Electrochem. Sci., 13: 2118-2125.
05. Chen, Q., H. Liu, Y. Xin and X. Cheng, 2013. TiO_2 nanobelts-effect of calcination temperature on optical, photoelectrochemical and photocatalytic properties. Electrochimica Acta, 111: 284-291.
06. He, F., F. Ma, J. Li, T. Li and G. Li, 2014. Effect of calcination temperature on the structural properties and photocatalytic activities of solvothermal synthesized TiO_2 hollow nanoparticles. Ceramics Int., 40: 6441-6446.
07. Ba-Abbad, M.M., A.A.H. Kadhum, A.B. Mohamad, M.S. Takriff and K. Sopian, 2012. Synthesis and catalytic activity of TiO_2 nanoparticles for photochemical oxidation of concentrated chlorophenols under direct solar radiation. Int. J. Electrochem. Sci., 7: 4871-4888.
08. Santhi, K., M. Navaneethan, S. Harish, S. Ponnusamy and C. Muthamizhchelvan, 2020. Synthesis and characterization of TiO_2 nanorods by hydrothermal method with different pH conditions and their photocatalytic activity. Applied Surface Sci., Vol. 500, 10.1016/j.apsusc.2019.144058-
09. Nikhil, A., D.A. Thomas, S. Amulya, S.M. Raj and D. Kumaresan, 2014. Synthesis, characterization and comparative study of CdSe-TiO_2 nanowires and CdSe-TiO_2 nanoparticles. Solar Energy, 106: 109-117.
10. Kim, C.S., B.K. Moon, J.H. Park, S.T. Chung and S.M. Son, 2003. Synthesis of nanocrystalline TiO_2 in toluene by a solvothermal route. J. Crystal Growth, 254: 405-410.